The Access Delay of Aloha with Exponential Back-off Strategies

Luca Barletta, Flaminio Borgonovo, and Ilario Filippini
Dipartimento di Elettronica, Informazione e Bioingegneria
Politecnico di Milano
I-20133 Milan, Italy
{luca.barletta, flaminio.borgonovo, ilario.filippini}@polimi.it

***Abstract*—This paper provides definite results about the access delay of slotted Aloha with exponential back-off, an infinite number of stages, and queues in saturation. The analysis is performed leveraging a method recently introduced, which indicates a maximum throughput equal to 0.370 with binary back-off, and 0.4303 when the exponential back-off base is optimized, and using a delay offset equal to 2. Here we provide the exact cumulative distribution of the access delay, showing the heavy-tail behavior already conjectured by using approximate models. We also prove that the existence of k-th order delay moments depends on explicit conditions on the number of stations involved and other system parameters as well.**

***Index Terms*—Slotted Aloha, Exponential Back-off, Collision Resolution, Access Delay, Decoupling Assumption, Random Access.**

I. Introduction

The Aloha protocol, since its appearance in 1970 [1], has been perhaps the most studied topic in the multiple-access area. Its applications cover important fields such as satellite, cellular and local-area communications, and recently has been applied to radio frequency identification (RFID). Its relevance to the present days is testified by the number of IEEE journal papers with "Aloha" in their title, which amount to 9 in the first four months of 2016 alone.

Here we deal with the performance of the slotted Aloha (S-Aloha) protocol using the exponential back-off (EB) with an infinite number of stages, and prove further results in the wake of the recent work presented in [2].

It has early been recognized that, in order to stabilize S-Aloha, the re-transmission probability at each station must be adapted to the number of active stations [3]. If no such information is available, the only way is to adapt the re-transmission probability to the station's own history. The only mechanism of this type so far considered, and called *backoff* [4], reduces the retransmission probability $\beta(i)$ as the number of collisions i suffered by the packet increases, on the ground that the number of suffered collisions measures the channel congestion degree. The mechanism most often referred to is the EB, which decreases the station transmitting probability according to the negative exponential law

$$\beta(i) = b^{-i-i_0}, \tag{1}$$

where $i \geq 0$ counts the number of consecutive collisions experienced in transmitting a packet, $b > 1$, and i_0 is the delay offset.

Definite results exist about stability and capacity of S-Aloha when channel feedback is available [5], [6], however no definite results have ever been presented for the EB case, although the latter's relevance to IEEE 802.3 and IEEE 802.11 standards have solicited a number of papers that appeared in the literature, for which the relevant reference is given in [2]. Among the most relevant results is the one in [7], where the author assumes that users arrive, transmit their packet according to law (1) with $i_0 = 0$, and after success leave. He proves that, with these parameters, the binary EB (BEB) asymptotically provides zero throughput under any positive packet arrival rate λ. Subsequent papers have tried to analyze the finite population model, although, due to the complexity of an exact analysis, only special models and approximations have been considered.

The most successful approximated model introduced so far is the saturation model of [8]. This model is used to analyze stability and capacity issues by assuming that queues are always full, thus implying that upon a successful transmission, immediately a new one is available for transmission at the same station. This model is somewhat simpler and pessimistic with respect to the one with queues, and has been adopted in the hope that it presented a stable behavior and positive capacity, thus guaranteeing these properties of the more realistic one.

With the saturation model, an approximate analysis is made possible by a further strong assumption, first introduced in [8], and then largely used, known as the *decoupling assumption*. This assumption has a twofold implication, *i.e.*, the *stationary* behavior of the model, and the *independence* in the behavior of the different transmitters. These assumptions lead to a mean value analysis (MVA) and a fixed point equation [8], that provides in a simple way the basic performance figures of the protocol. This model has been also adopted in [9] in order to derive throughput results for S-Aloha, and in [10] to study access delay.

Recently, in [2], we have addressed the capacity of S-Aloha protocol with EB in the variation that considers an infinite number of back-off stages and, in order to maximize the throughput, a small offset i_0. There, at first we have proven that the results attained by the decoupling assumption can be exactly re-derived assuming that the distribution of users

among the different stages is jointly Poisson. The advantage is that the Poisson model immediately provides all the results of the decoupling assumption, *e.g.*, those derived in [9]: hence, the *decoupling assumption* is hereafter referred as the *Poisson model*. The main result in [2], however, is a new semi-Poisson model (SPM) that provides a lower bound to the maximum throughput of the real system, which can be adjusted to closely approximate the protocol's maximum throughput. In particular, the model provides for BEB and $i_0 = 2$ a capacity close to 0.3706, slightly greater than e^{-1}, and 0.4303 when the exponential base is optimized to $b = 1.35$.

In this paper we extend the work in [2] by studying the access delay. In particular, we provide the complementary cumulative distribution function (CCDF) of the access delay, show that its tail decreases polynomially, with an exponent that depends on number of users N, the back-off base b, and the initial offset i_0. In particular, at capacity, the CCDF tail decreases as the first power of the delay. We re-derive the conditions given in [10] for the existence of the k-th moment under the decoupling assumption, and explicitly provide these conditions as function of N and other parameters.

The paper is organized as follows. In Section II we resume the basic result related to the decoupling assumption and the SPM. In Section III we analyze the access delay, and provide numerical results. Conclusions are drawn in Sec. IV.

II. Preliminary Results

The system is described by the Markov chain $(N_0, N_1, \ldots, N_i, \ldots)$, where N_i denotes the number of users with back-off index i. In the following, unless otherwise assumed, the expectations are taken with respect to the actual joint stationary distribution of the N_i's. The throughput of stage i can be expressed as

$$s_i = \mathsf{E}\left[\gamma_i(1, N_i) \prod_{k=0, k\neq i}^{\infty} \gamma_k(0, N_k)\right], \tag{2}$$

where

$$\gamma_i(k, N_i) = \binom{N_i}{k} \left(b^{-i-i_0}\right)^k \left(1 - b^{-i-i_0}\right)^{N_i - k}$$

is the probability of having k transmissions in stage i. The throughput is evaluated as

$$\lambda_0 = \sum_{i=0}^{\infty} s_i.$$

The rate of the flow of users across stage i is $\lambda_i = \lambda_{i-1} - s_{i-1},\ i \geq 1$, and the "routing" probability out of stage i, defined as $\alpha_i = \frac{\lambda_{i+1}}{\lambda_i}$, is given by:

$$1 - \alpha_i = \frac{s_i}{\lambda_i} = \frac{s_i}{\mathsf{E}\left[N_i\right] b^{-i-i_0}}, \tag{3}$$

where the last passage comes from Little's result [11]. We also have

$$\lambda_i = \lambda_0 \alpha_0 \alpha_1 \ldots \alpha_{i-1}, \qquad i \geq 1, \tag{4}$$

and again using Little's result, we can express N as

$$N = \sum_{i=0}^{\infty} \lambda_i T_i = \sum_{i=0}^{\infty} \lambda_i b^{i+i_0}, \tag{5}$$

where $T_i = b^{i+i_0}$ represents the average time a user spends in stage i. By the ratio test, the convergence of (5) requires

$$\lim_{i\to\infty} \frac{\lambda_{i+1}}{\lambda_i} = \lim_{i\to\infty} \alpha_i < 1/b.$$

Another interesting result is that the system can reach the steady state only if

$$P(\text{idle}) > \frac{b-1}{b}, \tag{6}$$

where $P(\text{idle})$ represents the probability that the channel is idle. In [2] we have shown that at capacity we have

$$\lim_{i\to\infty} \alpha_i = b^{-1}. \tag{7}$$

Other results, not only analytical but also numerical investigations, are prevented by the complexity of the Markov chain $(N_0, N_1, \ldots, N_i, \ldots)$, which has an infinite number of dimensions, each of them with an infinite number of states. Hence, to derive capacity results, some approximations must be introduced.

A. Poisson Model

The Poisson Model assumes that the stationary distribution of $(N_0, N_1, \ldots, N_i, \ldots)$ is jointly Poisson, independent from stage to stage. In [2] we have proved that this model provides, in a straightforward way, exactly the same results that have been derived in [9] under the decoupling assumption and a uniform back-off window. Below we summarize these results.

Denoting by $\Lambda = \sum_{k=0}^{\infty} \lambda_k$ the average traffic on the channel, we have

$$\alpha_i = \alpha = 1 - e^{-\Lambda}, \quad \lambda_i = \lambda_0 (1 - e^{-\Lambda})^i, \tag{8}$$

$$\lambda_0 = \Lambda e^{-\Lambda}, \tag{9}$$

$$N = b^{i_0} \frac{\Lambda e^{-\Lambda}}{1 - b(1 - e^{-\Lambda})}, \tag{10}$$

$$\Lambda < \ln \frac{b}{b-1}, \qquad P(\text{idle}) > \frac{b-1}{b}, \tag{11}$$

$$\lambda_0 < \frac{b-1}{b} \ln \frac{b}{b-1}.$$

The maximum throughput with $b = 2$ is $\ln(2)/2 \approx 0.34$, and e^{-1} for the optimized value of $b \approx 1.52$.

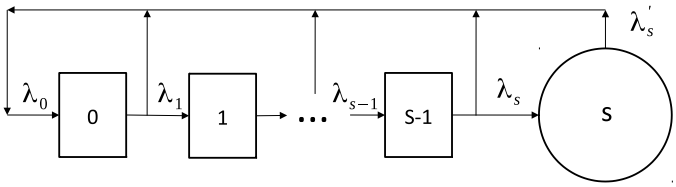

Figure 1. Scheme of the SPM with stages $0, 1, \ldots s-1$, and the lumped stage modeled with a Poisson distribution.

B. Semi-Poisson Model

The SPM, introduced in [2], assumes that starting from index $s > 0$, the stationary distribution of $(N_s, N_{s+1}, \ldots)$ is jointly Poisson distributed with averages $(n_s, n_{s+1}, \ldots)$. Therefore, the distribution of the number of transmitting users with index $i \geq s$ is given by the Poisson distribution with average

$$\Lambda_s = \sum_{i=s}^{\infty} \lambda_i = \sum_{i=s}^{\infty} n_i b^{-i-i_0}. \tag{12}$$

This shows that stages $s, s+1, \cdots$, from the transmission point of view, can be lumped together into a single enlarged stage s, as shown in Fig. 1. Assuming Λ_s as a known constant, we can numerically determine the behavior of the Markov process $(N_0, N_1, \ldots, N_{s-1})$, whose stationary distribution and cumulative average

$$n^{(<s)} = \sum_{i=0}^{s-1} \mathsf{E}\left[N_i\right]$$

depend on Λ_s.

We have also proven that the following relationship holds:

$$\Lambda_s = (N - n^{(<s)}) b^{-s-i_0} \left(b - \frac{b-1}{P(\text{idle})} \right), \tag{13}$$

where $P(\text{idle}) = \tau_s e^{-\Lambda_s}$, and

$$\tau_s = \mathsf{E}\left[\prod_{i=0}^{s-1} \gamma_i(0, N_i) \right],$$

where the average is taken over the stationary joint distribution of $(N_0, N_1, \ldots, N_{s-1})$.

Relationship (13) makes the system determined for a given N: For a fixed value of Λ_s, the statistics $n^{(<s)}$ and $P(\text{idle})$ can be determined by computing the stationary distribution of $(N_0, N_1, \ldots, N_{s-1})$ according to the SPM. If the left-hand side and the right-hand side of (13) match, then the sought value of Λ_s is found, otherwise we have to repeat the procedure for another value of Λ_s. Once Λ_s is found, the throughput can be evaluated as

$$\lambda_0 = e^{-\Lambda_s} \sum_{j=0}^{s-1} \mathsf{E}\left[\gamma_j(1, N_j) \prod_{k=0, k\neq j}^{s-1} \gamma_k(0, N_k) \right] + \Lambda_s e^{-\Lambda_s} \mathsf{E}\left[\prod_{k=0}^{s-1} \gamma_k(0, N_k) \right],$$

and

$$1 - \alpha_i = \frac{e^{-\Lambda_s} \mathsf{E}\left[\gamma_i(1, N_i) \prod_{k=0, k\neq i}^{s-1} \gamma_k(0, N_k) \right]}{\mathsf{E}\left[N_i\right] b^{-i-i_0}}, i < s \tag{14}$$

$$1 - \alpha_s = 1 - \alpha = e^{-\Lambda_s} \mathsf{E}\left[\prod_{k=0}^{s-1} \gamma_k(0, N_k) \right] = P(\text{idle}). \tag{15}$$

The chain represented by the SPM presents a number of states that increases exponentially with s. Luckily, the throughput provided by stage s decreases quickly as s increases, so that in [2] we have derived throughput results, even at capacity, with $s = 5, 6$. In Sec. III we show that the access delay CCDF is dominated by the asymptotic value of α_i, which can not be reached by the values of s used in [2]. Hence, means to get results with sensibly larger value of s have been devised.

With the SPM the space of $(N_0, N_1, \ldots, N_{s-1})$ has potentially an infinite number of stages; however, since the average of such components is very low (≈ 1.5), we have limited the size of each component to $N_{\max} \approx 5, 6 < N$ for large N, giving rise to a state space cardinality equal to $(N_{\max} + 1)^s$. For small N, the constraint $\sum_{i=0}^{s-1} N_i \leq N$ has been enforced, which results in a number of states equal to

$$\binom{N+s}{s}, \tag{16}$$

much smaller than $(N_{\max} + 1)^s$ for $N < (N_{\max})^s$.

III. Access-Delay Analysis

The access delay D is the time interval between two consecutive accesses by the same user. It can be evaluated as

$$D_R = \sum_{k=0}^{R} T_k, \tag{17}$$

where T_k is the geometric random variable (RV) that represents the time spent in stage k by a user, and R is the random index of the stage where the transmission is successful.

The throughput λ_0, evaluated as described in the previous section, immediately provides the first-order delay moment as

$$\mathsf{E}\left[D_R\right] = \frac{N}{\lambda_0}. \tag{18}$$

As simple as it is, relation (18) has been overlooked in many of the works appeared in the literature. It is readily proved by Little's Result and by observing that the throughput of each user is λ_0/N. On the other side, with the saturation model, the average number in the transmission buffer is always one. This result shows that the setting that provides the highest throughput, also gives the smallest average access delay.

The CCDF of D_R can be evaluated as

$$P(D_R > d) = \sum_{r=0}^{\infty} P(R = r) P(D_r > d), \tag{19}$$

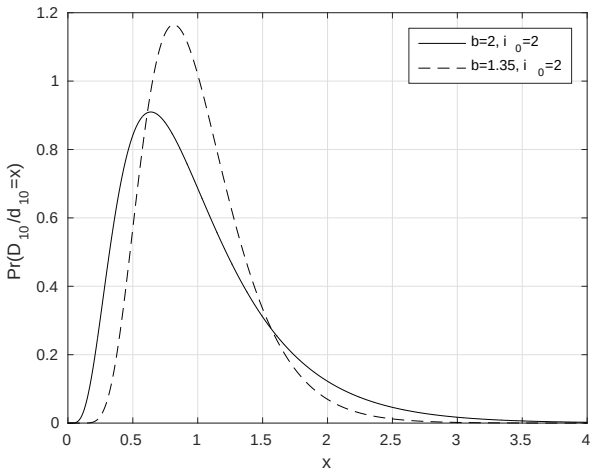

Figure 2. Probability distribution of D_r/d_r with $r = 10$ in the two cases $b = 2$ and $b = 1.35$ and offset $i_0 = 2$.

where the probability mass function of R, by (3) and (4), is

$$P(R = i) = \begin{cases} 1 - \alpha_0 & i = 0, \\ \alpha_0\alpha_1 \dots \alpha_{i-1}(1 - \alpha_i) & i \geq 1. \end{cases} \quad (20)$$

Conditioned to $R = r$, the probability mass function of D_r can be evaluated by taking the inverse Fourier transform of the characteristic function

$$G_{D_r}(e^{-\iota\omega}) \triangleq \mathsf{E}\left[e^{-\iota\omega D_r}\right] = \prod_{k=0}^{r} \frac{b^{-i_0-k}e^{-\iota\omega}}{1-(1-b^{-i_0-k})e^{-\iota\omega}}, \quad (21)$$

which follows by the conditional independence of the T_k's given $R = r$. Figure 2 shows the probability distribution of D_r/d_r with $r = 10$ in the two cases $b = 2$ and $b = 1.35$ and offset $i_0 = 2$, where

$$d_r = \mathsf{E}\left[D_r\right] = \sum_{k=0}^{r} b^{k+i_0} = b^{i_0}\frac{b^{r+1}-1}{b-1} \approx \frac{b^{i_0+r+1}}{b-1}, \quad (22)$$

the last approximation holding true for large r. Evaluations of D_r/d_r for values of $r > 10$ show no changes, so we have the following

Proposition 1: *For $r \to \infty$ the distribution of D_r/d_r is independent of r.*

This property can be used to show that for any suitably large $d = x_r\, d_r$ two values of r exist, namely r_1 and r_2, such that

$$P\left(\frac{D_r}{d_r} > x_r\right) \approx 0, \qquad r < r_1 \quad (23)$$

$$P\left(\frac{D_r}{d_r} > x_r\right) \approx 1, \qquad r > r_2. \quad (24)$$

Using (23) and (24) simplifies (19) into

$$P(D_R > d) \approx \sum_{r=r_1}^{r_2} P(R = r)P\left(\frac{D_r}{d_r} > x_r\right) + P(R > r_2), \quad (25)$$

Table I
RELEVANT TERMS IN THE ASYMPTOTIC CCDF OF D_r/d_r, FOR $b = 2$ AND $b = 1.35$ WITH $i_0 = 2$.

r	f_r	$b = 2$	$b = 1.35$
$i-2$	$P\left(D_r/d_r > b^2\right)$	0.0011	0.0352
$i-1$	$P\left(D_r/d_r > b\right)$	0.0623	0.1665
i	$P\left(D_r/d_r > 1\right)$	0.4055	0.4345
$i+1$	$P\left(D_r/d_r > b^{-1}\right)$	0.8259	0.8701
$i+2$	$P\left(D_r/d_r > b^{-2}\right)$	0.9793	0.9135

which can finally be used to get numerical results.

Next we show how to evaluate the tail of the CCDF of D_R. To this purpose, we focus on the CCDF at delay d_i, which by (25) and (22) can be written as

$$P(D_R > d_i) \approx \sum_{r=r_1}^{r_2} P(R = r)P\left(\frac{D_r}{d_r} > b^{i-r}\right) + P(R > r_2). \quad (26)$$

Table I reports the values $P(D_r/d_r > b^{r-i})$ that are relevant to the summation in (26), that refer to values $r_1 = i - a$, $r_2 = i+b$, being a and b constant dependent on the parameters. For large i we can exploit the fact that in (20), as shown by the analysis synthesized in sec. II, we have

$$\lim_{i\to\infty} \alpha_i = \alpha. \quad (27)$$

Assuming that for $i \geq u$ we have $\alpha_i \approx \alpha_u \approx \alpha$, and denoting $\alpha_0\alpha_1 \dots \alpha_{u-1}/(\alpha_u)^u = \mu_u$, we can write

$$P(R = r) = \mu_u(1 - \alpha_u)\alpha_u^r, \qquad r \geq u,$$
$$P(R > r) = \mu_u\alpha_u^{r+1}, \qquad r \geq u.$$

By substituting the above distribution, and using the values in Table I, (26) becomes

$$P(D_R > d_i) \approx A\alpha_u^i, \qquad i \geq u + 2, \quad (28)$$

where

$$A = \mu_u(1 - \alpha_u)\Bigg[\alpha_u^{-2}f_{i-2} + \alpha_u^{-1}f_{i-1} + f_i + \alpha_u f_{i+1} + \alpha_u^2\left(f_{i+2} + \frac{\alpha_u}{1-\alpha_u}\right)\Bigg].$$

The asymptotic value α_u is an increasing function of N, that we write as

$$\alpha_u = b^{-\zeta(N)}, \quad (29)$$

where $\zeta(N) > 1$ is a decreasing function of N, reaching 1 at $N = \infty$ (7). Using (29) into (28) we have

$$P(D_R > d_i) \approx A(b, \zeta)b^{-\zeta i}. \quad (30)$$

From (22) we get

$$d_i^\zeta \approx \left(\frac{b^{i_0+1}}{b-1}\right)^\zeta b^{\zeta i},$$

which used into (30) provides

$$P(D_R > d_i) \approx A(b, \zeta)\left(\frac{b^{i_0+1}}{b-1}\right)^\zeta d_i^{-\zeta}. \quad (31)$$

Although (31) is defined only at values d_i, we assume its extension to the continuous axis to provide the CCDF of D_R:

$$P(D_R > d) \approx H(b, \zeta, i_0) d^{-\zeta}. \tag{32}$$

Since (32) is represented by a straight line in a log-log scale, we dub ζ *the slope* of the tail.

What proved above can be resumed by the following

Proposition 2: *The tail of the CCDF of the access delay decreases polynomially in d, with slope $\zeta(N)$ that decreases with N.*

From distribution (32) we can derive the moments of D_R as

$$\begin{aligned} \mathsf{E}\left[(D_R)^k\right] &= \int_0^\infty k d^{k-1} P(D_R > d)\, \mathrm{d}\, d \\ &\approx H(b, \zeta, i_0) \int_0^\infty k d^{-(\zeta - k + 1)}\, \mathrm{d}\, d. \end{aligned} \tag{33}$$

We see that the condition for the existence of such moments is

$$\zeta > k. \tag{34}$$

Condition (34) can be expressed in terms of the collision probability α_u as

$$\alpha_u < b^{-k}. \tag{35}$$

Since α_u depends on N, we can also express condition (34) in terms of N or channel traffic Λ.

We also have the following

Proposition 3: *The CCDF tail has slope $\zeta = 1$ at capacity, and $\zeta = i_0$ for $N = 2$.*

In fact, (7) shows that at capacity we have $\alpha_u = 1/b$, which, by (29), provides $\zeta = 1$, independent of b. We see also that with $N = 2$, the only state that has probability close to one, when a user is in a stage $u \gg 1$, is the one with $N_0 = 1$. In these conditions we have

$$\alpha_u = b^{-i_0}, \tag{36}$$

which provides $\zeta = i_0$.

Proposition 3 shows that by using $i_0 = 2$ we do not have any second order moment for $N \geq 3$. In any cases, with large N, as it happens close to capacity, ζ tends to one, so that no second order moment can exist for any i_0 and b.

We note that all the results stated by Propositions 1, 2, and 3, with the exception for the case $N = 2$, can be derived in the same way with the Poisson model, where α_i is assumed constant. We notice, however, that using the Poisson model with $N = 2$, by (8) and (10) we get $\alpha = 0.27$ and $\zeta = 1.89$. Hence, once again, we see that the Poisson model is pessimistic.

A. Numerical Evaluations

A suitable value for α_u can be evaluated by (14) in the SPM, using $u = s - 1$, *i.e.*, the highest stage of the model, not considering the lumped stage. We do not consider (15) since this represents $P(\text{idle})$, *i.e.*, the probability that all users are silent, although for large N (14) and (15) tend to coincide.

Table II
EXACT AND ESTIMATED ASYMPTOTIC SLOPES $\zeta = -\log_b(\alpha_{s-1})$ FOR DIFFERENT VALUES OF N.

		$N=2$	$N=3$	$N=5$	$N=10$	$N=\infty$
$i_0=2$	$b=2$	2	1.5331	1.289	1.131	1
$i_0=2$	$b=1.35$	2	1.433	1.219	1.213	1
$i_0=6$	$b=2$	6	5.059	4.108	3.095	1

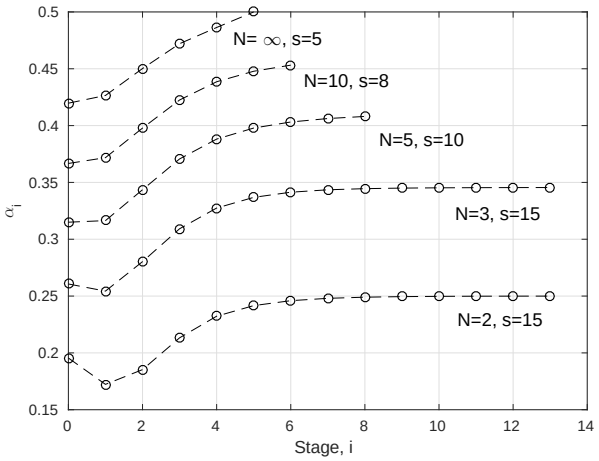

Figure 3. Values of the sequence α_i versus i up to $i = s - 1$ for $N = \{2, 3, 5, 10, \infty\}$, $i_0 = 2$, and $b = 2$.

Then, assuming $\alpha_i = \alpha_u = \alpha_{s-1},\ i \geq s$, we can use (20) and (25) to numerically evaluate the CCDF for large d.

In order to guarantee that α_{s-1} in (14) represents the sought asymptotic value, we must verify that sequence α_i settles into an asymptote equal to α_{s-1}. Figure 3 shows the sequence α_i versus i up to $i = s - 1$ for $N = \{2, 3, 5, 10, \infty\}$, $i_0 = 2$, and $b = 2$. As we can see, the convergence to an asymptote is guaranteed for $N \leq 5$, while for $N \geq 10$ the maximum s allowed by the computational complexity presents a small error. For $N = \infty$ we let $\alpha_5 = 0.5$, which is the asymptotic value predicted by (7).

The slopes ζ corresponding to estimated asymptotic values α_{s-1} are reported in Table II, for different values of b and i_0. Values for $N = 2$ and $N = \infty$ represent the exact values provided by the analysis and are the same for all values of b. For different values of N, however, b influences ζ, although for a small amount. Finally, the case with $i_0 = 6$ shows that higher moments of the delay exist with this offset, as shown in Table II.

The CCDF of D_R for the cases $N = \{2, 3, 5, 10, \infty\}$, with parameters $b = 2$ and $i_0 = 2$, is shown in Fig. 4, where we have used the characteristic function (21) to evaluate the probabilities for small delays, and the values α_i depicted in Fig. 3 to compute the tails.

We notice again that for $N = 2$ and $N = \infty$ exact slopes are provided by the analysis, while in the other cases we have used the approximated solution provided by the SPM. The approximation encounters its limit in the maximum value of s allowed by the numerical complexity, and diminishes as N increases. To validate the curves we have also reported

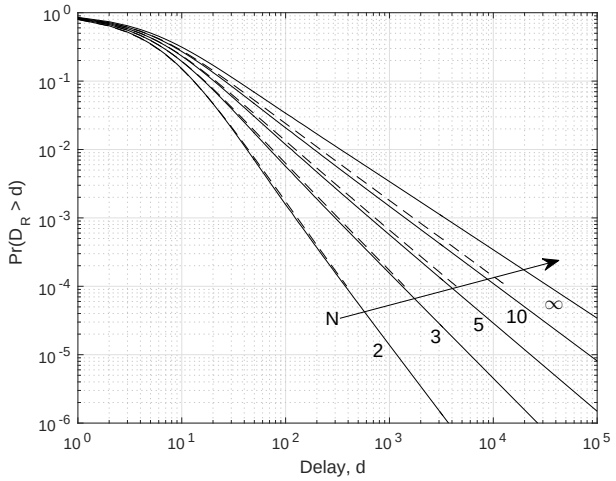

Figure 4. The complementary cumulative distribution function of the access delay D_R for the cases $N = \{2, 3, 5, 10, \infty\}$, with parameters $b = 2$ and $i_0 = 2$. Solid line: analytic evaluation. Dashed line: Monte Carlo simulation.

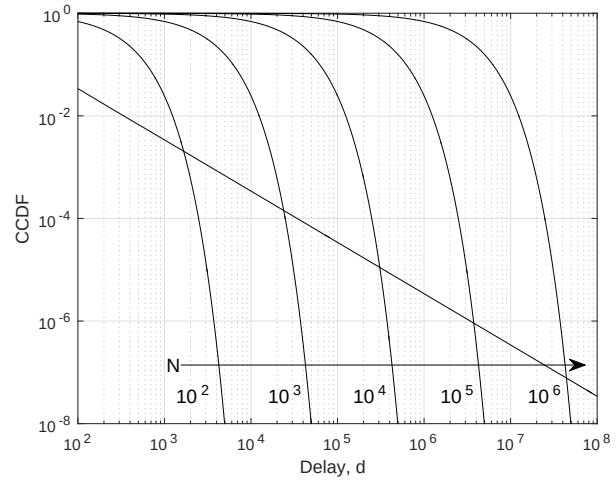

Figure 5. Comparison between the complementary cumulative distribution function of BEB and of the geometric delay for values $N = \{10^2, 10^3, 10^4, 10^5, 10^6\}$.

the dashed lines representing the sample CCDF's derived by simulating the BEB for 5×10^8 time slots, and for moderate values of N. As we can see, the measured results almost perfectly match with the evaluations attained by SPM. The small mismatch observed for $N = 5, 10$ can not be safely ascribed either to lack of approximation of SPM or to slow convergence of the simulation.

As predicted by (32), the tails of the distributions are represented, in the log-log scale, by straight lines of constant slope, which decreases as N increases. In any cases, the heavy-tail behavior of the delay distribution is confirmed. This behavior is known as *short term unfairness*, and represents the fact that users with low indexes are by far more advantaged with respect to others in re-accessing the channel. This causes a short term capture of the channel by low index users that causes very long access delays to other users. The short term capture is absent when all users have the same probability of accessing the channel, and this results in a geometric distribution of the access delay with parameter λ_0/N, the reciprocal of the average delay. We show in Fig. 5 the comparison between the BEB CCDF and the CCDF of the geometric delay just cited, for values of $N = \{10^2, 10^3, 10^4, 10^5, 10^6\}$. For the BEB case we have reported only the CCDF at capacity, *i.e.*, $N = \infty$, since all the curves for the cited N are almost indistinguishable from the latter. We see that, almost in balance of the short term unfairness, the exponential back-off distribution lies well below the geometric one for a great range of delay values, guaranteeing fast access to an high percentage of transmissions, which the geometric one can not guarantee, and this even with $N = \infty$.

Before ending this section we must notice that the result on moments, expressed in the implicit form (35), has already been derived in [10] referring to the IEEE 802.11 DCF access protocol, and window-type back-off. This is not an incident since the basic throughput-delay results of IEEE 802.11 derived there, can be easily re-conducted to the Slotted Aloha protocol here considered. Furthermore, those results have been attained using the decoupling assumption, which provides a pessimistic slope at small N.

IV. Conclusions

In this paper we have explicitly derived some results about the access delay for the Aloha protocol, with exponential back-off mechanism and queues in saturation. We have been able to evaluate the delay cumulative distribution, whose tail decreases polynomially, with an exponent that changes with the number of users, in the range $[1, i_0]$. The results also show that for $i_0 \leq 2$ no second moment exists, thus explaining the behavior known as short term unfairness.

References

[1] N. Abramson, "The Aloha system: Another alternative for computer communications," in *Proc. Fall Joint Computer Conf.*, vol. 37, Nov. 1970, pp. 281–285.

[2] L. Barletta, F. Borgonovo, and I. Filippini, "The S-aloha capacity: Beyond the e^{-1} myth," in *Proc. INFOCOM 2016*, 2016. [Online]. Available: ftp://ftp.elet.polimi.it/outgoing/Flaminio.Borgonovo/PUBBL/2016-infocom.pdf

[3] G. Fayolle, E. Gelenbe, and J. Labetoulle, "Stability and optimal control of the packet switching broadcast channel." *Journal of ACM*, vol. 24, no. 3, pp. 375 – 386, Jul. 1977.

[4] R. M. Metcalfe and D. R. Boggs, "Ethernet: Distributed packet switching for local computer networks," *Commun. ACM*, vol. 19, no. 7, pp. 395–404, Jul. 1976.

[5] R. L. Rivest, "Network control by Bayesian broadcast," *IEEE Trans. Inf. Theory*, vol. 33, no. 3, pp. 323–328, May 1987.

[6] L. P. Clare, "Control procedures for slotted Aloha systems that achieve stability," in *Proceedings of the ACM SIGCOMM Conference on Communications Architectures & Protocols*, 1986, pp. 302–309.

[7] D. J. Aldous, "Ultimate instability of exponential back-off protocol for acknowledgment-based transmission control of random access communication channels," *IEEE Trans. Inf. Theory*, vol. 15, no. 2, pp. 219–223, Mar. 1987.

[8] G. Bianchi, "Performance analysis of the IEEE 802.11 distributed coordination function," *IEEE J. Select. Areas Commun.*, vol. 18, no. 3, pp. 535–547, March 2000.

[9] B.-J. Kwak, N.-O. Song, and L. Miller, "Performance analysis of exponential backoff," *IEEE/ACM Trans. Netw.*, vol. 13, pp. 343–355, April 2005.

[10] T. Sakurai and H. Vu, "Mac access delay of IEEE 802.11 DCF," *IEEE Trans. Wirel. Commun.*, vol. 6, no. 5, pp. 1702–1710, May 2007.

[11] J. D. C. Little, "A proof for the queuing formula: L= λ W," *Operations Research*, vol. 9, no. 3, pp. 383–387, 1961.